Reentrant Mound Formation in GaAs(001) Homoepitaxy Observed by *ex situ* Atomic Force Microscopy

Georgios Apostolopoulos,* Jens Herfort, Lutz Däweritz, and Klaus H. Ploog
Paul-Drude-Institut für Festkörperelektronik, Hausvogteiplatz 5-7, D-10117 Berlin, Germany

Martina Luysberg
Institut für Festkörperforschung, Forschungszentrum Jülich, D-52425 Jülich, Germany
(Received 1 October 1999)

A study of the surface morphology of homoepitaxial GaAs(001) by means of *ex situ* atomic force microscopy in air reveals the reentrance of mounding behavior at low growth temperatures. A transition from statistical roughening to organized mound formation is observed as the growth temperature is reduced. We show by means of growth simulations that the observed morphology is compatible with anisotropic adatom diffusion in the presence of an Ehrlich-Schwoebel barrier. The mechanism leading to this kind of adatom kinetics at low temperatures is interpreted in terms of surfactant acting arsenic condensing on the surface.

PACS numbers: 68.35.Bs, 68.35.Fx, 81.15.Hi

A number of recent experimental investigations [1–3] on epitaxial growth have shown that the formation of a fairly regular pattern of three-dimensional (3D) growth mounds on an initially flat surface is common to a broad range of material systems from metals to semiconductors, during homoepitaxy [1,2] as well as heteroepitaxy [3]. The origin of this phenomenon can be traced to an intrinsic growth instability of the singular surface in the presence of so-called Ehrlich-Schwoebel (ES) diffusion barriers [4], which inhibit the downward movement of adatoms at surface step edges. The influence of ES barriers on film growth was first discovered experimentally by Kunkel *et al.* [5]. The theoretical basis was laid by Villain [6], but it was Johnson *et al.* [1] who clearly demonstrated by simulation and experiment that the fate of an unstable singular surface is the eventual buildup of a mound pattern. The physical implication of the ES barrier is that adatoms are hindered in stepping down from a terrace (although this would mean an energetically favorable incorporation at the step edge), resulting in increased probability of new 2D islands nucleating on already existing ones. The repetition of this process leads to the multilayer structures called growth mounds.

Apart from mound formation, ES barriers lead also to a rapid roughening of the growth front, thus preventing the observation of surface diffraction intensity oscillations, as for instance in reflection high-energy electron diffraction (RHEED). Such oscillations are generally associated with smooth layer-by-layer growth. However, by lowering the temperature, intensity oscillations are again observed, a phenomenon described as reentrant layer-by-layer growth [5]. The lower temperature limits the diffusivity of adatoms, thereby effectively reducing the consequences of ES diffusion barriers. Hence, layer-by-layer growth sets in again, assisted by other smoothing mechanisms like "downward funneling" [7], i.e., the spontaneous downward movement of atoms deposited directly on step edges or other microprotrusions of the surface.

In this Letter, we report on a new kind of reentrant behavior, regarding this time the formation of mounds, observed during homoepitaxy on GaAs(001). Mounding has already been studied in this system [1,8], however, only at the high growth temperature region ($\sim$550 °C). We find that at intermediate temperatures around 300 °C the growth front becomes smooth, while for $T < 260$ °C mounds dominate again the morphology. Comparison to growth simulations shows that the low temperature mound pattern is compatible with a high anisotropic adatom mobility in the presence of an ES barrier. The surprising enhancement of adatom diffusion at low temperatures is attributed to the previously reported effect of As condensing on the surface [9].

The GaAs films are grown by molecular-beam epitaxy (MBE) on nominally singular GaAs(001) substrates. Ga and As_4 molecular beams are supplied from solid source effusion cells, and their flux is controlled by measuring the beam equivalent pressure (BEP) with an ionization gauge. The native oxide layer is removed by heating the substrate to 580 °C for 30 min under As_4 overpressure. After oxide desorption, a 250 nm GaAs buffer layer is deposited at 580 °C at a As_4:Ga BEP ratio of 20. Growth is continued at a lower temperature after a $\sim$10 min interruption to allow for the substrate temperature to stabilize. Substrate temperatures in the 200–300 °C range are measured with a thermocouple, calibrated using the melting points of In and Sn.

The strain appearing in our low substrate temperature grown GaAs layers, examined by means of double crystal x-ray diffraction rocking curves, is in good agreement with recent reports [10]. Cross sectional transmission electron microscopy investigations reveal that the GaAs films are high quality single crystals with no structural defects. The surface morphology was examined *ex situ* by atomic force

 0031-9007/00/84(15)/3358(4)$15.00

microscopy (AFM) in the constant force mode. AFM measurements were carried out in air, therefore a thin oxide overlayer may be present on the sample surface. However, as has been shown in many previous reports [8,11], the surface oxide of GaAs does not affect significantly the AFM measurements.

Figures 1(a) and 1(b) are two typical AFM images exhibiting the behavior of the surface morphology with respect to growth temperature. The samples have a thickness of 1 μm and are grown under As-rich conditions (As_4:Ga BEP ratio $\approx$20). At temperatures higher than 260 °C [Fig. 1(a)] the surface is smooth with a surface width (roughness) of 1.5 nm, which is comparable to that of the buffer layer. However, monolayer steps cannot be resolved with the AFM on low substrate temperature grown samples, in contrast to the buffer layer which exhibits well-defined large one-monolayer high terraces of 160 nm average width. This is probably because the average terrace width in low temperature grown samples is below the resolution of the AFM. When the growth temperature is reduced, a pattern of growth mounds emerges as clearly seen in Fig. 1(b). The mounds have a height of 8 nm, lateral dimensions of $\sim$50 nm, and are elongated along $[\bar{1}10]$; they loosely organize in columns running parallel to $[\bar{1}10]$. With decreasing growth temperature the height of the mounds increases and they become more and more asymmetric. Similar effects are found also as a function of the As_4 overpressure prevailing during growth. Specifically, we observed that growth at $T = 210$ °C under a significantly lower BEP ratio of 8 (but still in the As-rich regime), leads to the disappearance of the mound pattern and to a surface morphology similar to Fig. 1(a).

In order to quantify our observations we calculate the height-height correlation function $G(x, y)$ from the AFM data. $G(x, y)$ is here given by the average $\frac{1}{2}\langle\tilde{h}(x + x', y + y')\tilde{h}(x', y')\rangle_{(x',y')}$, where $\tilde{h}(x, y)$ is the height at point (x, y) relative to the average height, i.e., $\tilde{h} = h - \langle h\rangle$ with $\langle\cdots\rangle$ denoting an averaging over the whole image area. x and y are parallel to [110] and $[\bar{1}10]$, respectively. The root-mean-square (rms) width is given by $w = \sqrt{G(0, 0)}$. The position of the first maximum of $G(x, 0)$ corresponds to the average distance between growth mounds along [110], thus, twice the mound radius R_m. Figure 2(a) shows $G(x, 0)$, normalized to w^2, as a function of x at various growth temperatures. At $T < 260$ °C the height-height correlation function exhibits oscillations which are characteristic for mound formation. The positions of the first maxima, denoted by arrows, shift to lower x values with decreasing temperature. At $T > 260$ °C, $G(x, 0)$ resembles the functional form $G \sim e^{-(x/\xi)^{2\zeta}}$, which is valid for small x in systems exhibiting kinetic roughening [12], with ξ and ζ representing the correlation length and roughening exponent, respectively. From our data we estimate $\zeta \approx 0.65$, which is consistent with the value of $2/3$ predicted from nonlinear growth equations describing kinetic roughening during MBE [13]. Figure 2(b) depicts the dependence on growth temperature of the mound radius R_m and slope w/R_m along [110]. R_m increases up to 40 nm at $T = 260$ °C. At this growth temperature the mounds have become almost symmetric and very flat. Accordingly, w/R_m decreases rapidly with increasing growth temperature.

Mounds are also elongated along $[\bar{1}10]$ at high temperatures [1], but have significantly larger lateral radii of $\sim$0.5 μm. One could suppose that mounds observed at lower temperatures are actually due to the same phenomenon, only smaller because of the reduced adatom diffusivity. However, if we take into account the value of 1.58 eV for the single adatom hopping barrier E_a on the GaAs(001) surface [14], then the thermal hopping rate $h \propto \exp(-E_a/k_BT)$ in our experiments is about 8 orders of magnitude smaller than in the high temperature case.

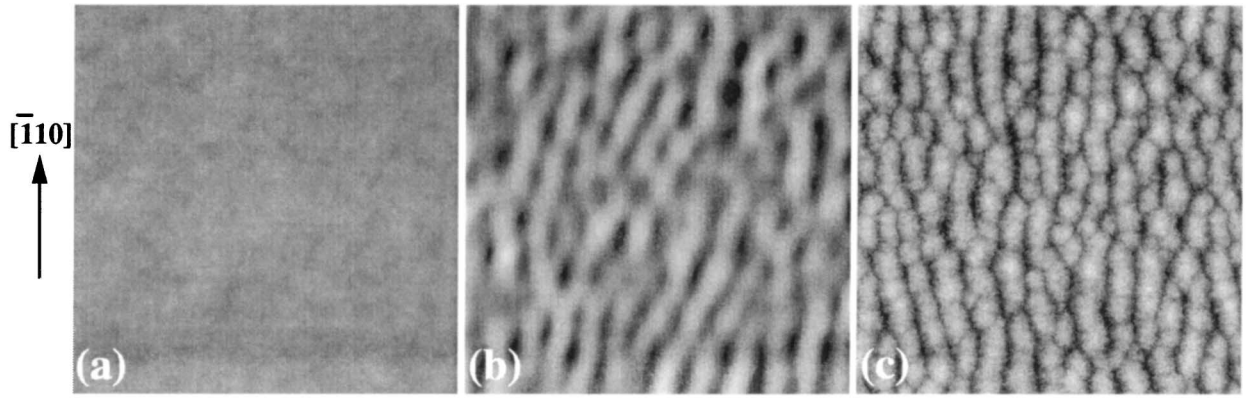

FIG. 1. (a) AFM image of a 1 μm thick GaAs(001) layer grown at a substrate temperature of 280 °C. The area of the image is 1×1 μm^2. (b) AFM image of a 1 μm thick GaAs(001) layer grown at 210 °C. The area of the image is 0.5×0.5 μm^2. Images (a) and (b) have the same gray scale contrast, which covers a height difference of 8.0 nm. (c) Gray scale image of the surface morphology obtained from growth simulation of a 1 μm thick GaAs layer. The diffusion length along [110] $\ell_d^{[110]}$ is 13.6 nm, the ratio $\ell_d^{[\bar{1}10]}/\ell_d^{[110]}$ is 0.75, and the Ehrlich-Schwoebel length, ℓ_{ES}, is 1.2 nm. The gray scale and area of the image cover 4.0 nm and 0.5×0.5 μm^2, respectively.

Thus, a drastic change in surface morphology should be expected. Furthermore, the above assumption cannot explain the reentrant behavior. Another issue which ought to be discussed regards the phenomenon of strain-induced roughening, which has been invoked to explain the morphology of strained $In_xGa_{1-x}As$ on GaAs(001) [15]. We believe that this effect is not relevant to our observations, due to the strain in our samples being considerably smaller ($\sim 0.1\%$) than in $In_xGa_{1-x}As$ layers ($\sim 7.2 \times x_{In}\%$). In contrast, the developed roughness is almost equally high in both cases. Considering all points mentioned above, we conclude that the reentrance of mounding in GaAs has to rely on a new adatom diffusion mechanism, which becomes significant only at temperatures below 260 °C. The new diffusion mechanism is also governed by an ES barrier, so that mound formation occurs anew. Furthermore, the presence of an As surplus during growth is essential, as mounding is observed only at high As_4:Ga BEP ratios.

In order to test these ideas, we perform numerical simulations based on discrete growth models employed previously to metal homoepitaxy [16]. Atoms are deposited randomly on the (001) surface of an fcc lattice and are finally incorporated at fourfold hollow (4FH) sites.

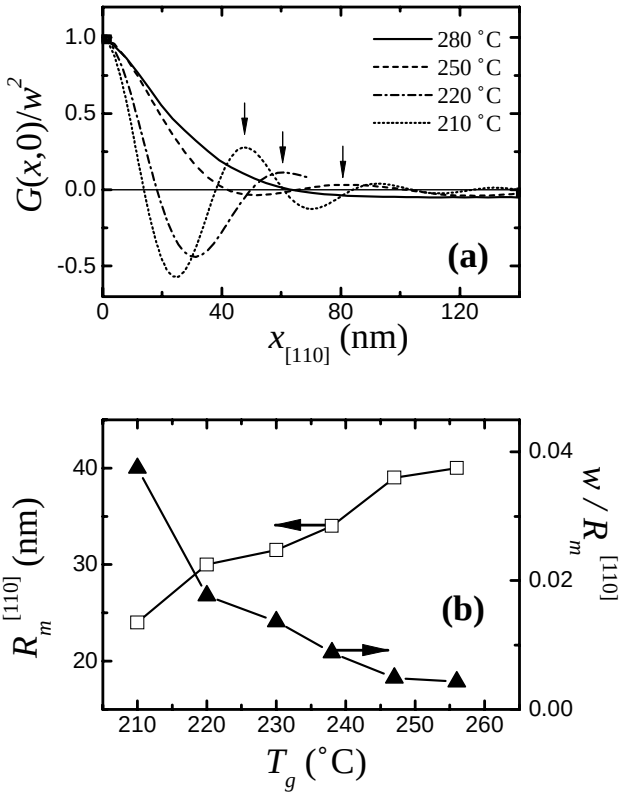

FIG. 2. (a) Height-height correlation functions normalized to the square of the surface width, $G(x,0)/w^2$, versus distance x along [110] obtained from AFM images of GaAs layers grown on GaAs(001) at various temperatures. Arrows denote the position of the first maximum of $G(x,0)$, which corresponds to twice the mound radius R_m. (b) Mound radius R_m and slope w/R_m along [110] as a function of growth temperature.

We consider only the group-III species kinetics, since we are interested in conditions where growth is limited by the supply of Ga. This justifies also the use of an fcc lattice, which represents the Ga sublattice. The model includes the mechanism of downward funneling [7]. This effect has been mainly used in metal homoepitaxy simulations [16], however, Šmilauer and Vvedensky [17] have shown that a similar incorporation mechanism is also essential for the description of GaAs homoepitaxy. Deposited adatoms with no next-nearest neighbors are allowed to move by hopping to neighboring 4FH sites. In order to be able to study the behavior of our model at large epitaxial thicknesses, the regime relevant to our experiments, we make the following simplifications: (i) each adatom is treated separately and (ii) adatoms are simulated as random walkers with a finite diffusion length ℓ_d [18]. These approximations are justified due to the high step density of a surface covered with growth mounds, which ensures that an adatom will be in most cases incorporated at a step edge before having the chance to meet another diffusing adatom. Incorporation of adatoms is considered irreversible due to the low temperature. As a measure of the ES barrier, E_{ES}, we define the length $\ell_{ES} \equiv a(R - 1)$, where R is the ratio of the probability for terrace hopping to the probability of hopping downward at a step edge. The distance between two 4FH sites is represented by a. For thermally activated hopping $R = \exp(E_{ES}/k_BT)$, so that ℓ_{ES} should decrease with increasing temperature.

Figure 1(c) shows a gray scale image of the surface morphology obtained by simulating the growth of 1 μm ($\sim$3600 monolayers) GaAs on an initially flat GaAs(001) surface. We used different diffusion lengths along [110] and [$\bar{1}$10] to account for the anisotropy observed in the experiment. The agreement with the experimental growth pattern is notable. It may seem surprising that mounds are elongated along the shortest diffusion length. This is happening because reduced diffusion along this direction results also in a weaker effect of the ES barrier. Thus, mound formation is not pronounced along [$\bar{1}$10]. Figure 3(a) depicts the height-height correlation function of simulated surfaces at different values of ℓ_{ES}, while Fig. 3(b) shows the corresponding values of R_m and w/R_m as a function of ℓ_{ES}^{-1}. The experimental behavior with respect to growth temperature may be reproduced by a rapidly increasing ℓ_{ES} with decreasing temperature. This behavior agrees with the definition of the ES length. The predicted values for R_m and w/R_m are realistic in comparison with the experimental ones. To our knowledge, this is the first time that results of kinetic simulations for the particular homoepitaxial system of GaAs/GaAs(001) are in good *quantitative* agreement with experiment. We assume that this is because a number of processes like diffusion along step edges, detachment from steps, and capillary-induced mound coalescence are quenched at low substrate temperatures, thus simplifying the physical description. Our simulation procedure allows only an indirect estimation of the hopping barriers. For the adatom hopping barrier E_a,

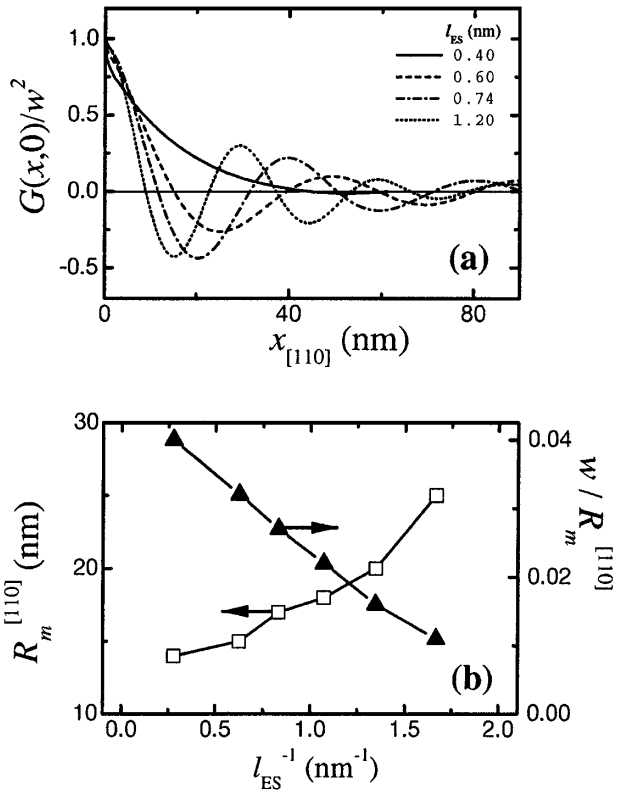

FIG. 3. (a) Height-height correlation functions normalized to the square of the surface width, $G(x,0)/w^2$, versus distance x along [110] obtained from simulated surfaces at different values of the Ehrlich-Schwoebel length ℓ_{ES}. (b) Mound radius R_m and slope w/R_m along [110] as a function of ℓ_{ES}^{-1} obtained from growth simulations.

we use the relation $\ell_d \approx a(h/f)^{1/6}$ [12], where f is the deposition rate and $h = (k_B T/\hbar)e^{-E_a/k_B T}$ the thermally activated hopping rate [14]. Setting $f \approx 1$ sec^{-1}, we find an E_a of $\sim$0.5 eV, significantly lower than the high temperature value cited above [14]. Furthermore, comparing the variation of ℓ_{ES} to the experimental temperature interval, we infer that E_{ES} lies between 0.05 and 0.1 eV.

A last remaining issue regards the origin of the enhanced adatom diffusion at low temperatures. It is obvious that a key role is played by the As_4 overpressure. Recently, it was proposed that As condensing on the GaAs(001) surface at low temperatures may act as a surfactant [9], i.e., as a surface-active species that modifies the growth mode [19]. This model was based on the observation of RHEED intensity oscillations at low growth temperatures. However, this effect might also be related to reentrant layer-by-layer growth cited above [5]. We believe that our findings on mound formation point now unambiguously to an As-controlled diffusion mechanism at low temperatures. Furthermore, our analysis provides an adequate explanation for the behavior of low temperature RHEED oscillations with respect to the BEP ratio as reported by Shen *et al.* [9]. These authors find that the oscillation intensity first increases and then decreases as the BEP ratio is increased. Our interpretation is that the initial increase of oscillation intensity is due to the As-induced enhancement of adatom diffusion. As the As_4 overpressure increases further, the effect of the ES barrier becomes also stronger, the surface roughens rapidly and RHEED oscillations are suppressed.

We are indebted to Rudolf Hey, Yukihiko Takagaki, and Matthias Wassermeier for enlightening discussions. Karin Hagenstein is gratefully acknowledged for assistance in sample preparation. Part of this work was supported by the German Bundesministerium für Bildung und Forschung (BMBF) under Contract No. 13N7088/0.

*Present Address: Institute of Materials Science, National Centre for Scientific Research "Demokritos," 153 10 Ag. Paraskevi, Attiki, Greece.

[1] M. D. Johnson *et al.*, Phys. Rev. Lett. **72**, 116 (1994).
[2] H.-J. Ernst *et al.*, Phys. Rev. Lett. **72**, 112 (1994); J. E. Van Nostrand *et al., ibid.* **74**, 1127 (1995); J. A. Stroscio *et al., ibid.* **75**, 4246 (1995); J.-K. Zuo and J. F. Wendelken, *ibid.* **78**, 2791 (1997).
[3] K. Thürmer *et al.*, Phys. Rev. Lett. **75**, 1767 (1995); F. Tsui *et al., ibid.* **76**, 3164 (1996).
[4] G. Ehrlich and F. G. Hudda, J. Chem. Phys. **44**, 1039 (1966); R. L. Schwoebel and E. J. Shipsey, J. Appl. Phys. **37**, 3682 (1966).
[5] R. Kunkel *et al.*, Phys. Rev. Lett. **65**, 733 (1990).
[6] J. Villain, J. Phys. I (France) **1**, 19 (1991).
[7] J. W. Evans *et al.*, Phys. Rev. B **41**, 5410 (1990).
[8] C. Orme *et al.*, Appl. Phys. Lett. **64**, 860 (1994).
[9] A. Shen *et al.*, Appl. Surf. Sci. **130**, 382 (1998); H. Yasuda and H. Ohno, Appl. Phys. Lett. **74**, 3275 (1999).
[10] M. Luysberg *et al.*, J. Appl. Phys. **83**, 561 (1998).
[11] R. Hey *et al.*, J. Cryst. Growth **154**, 1 (1995); F. Lelarge *et al., ibid.* **175/176**, 1087 (1997); F. Lelarge *et al., ibid.* **175/176**, 1102 (1997).
[12] A. L. Barabási and H. E. Stanley, *Fractal Concepts in Surface Growth* (Cambridge University Press, Cambridge, England, 1995).
[13] Z. W. Lai and S. Das Sarma, Phys. Rev. Lett. **66**, 2348 (1991).
[14] T. Shitara, J. H. Neave, and B. A. Joyce, Appl. Phys. Lett. **62**, 1658 (1993).
[15] C. W. Snyder *et al.*, Phys. Rev. Lett. **66**, 3032 (1991).
[16] M. C. Bartelt and J. W. Evans, Phys. Rev. Lett. **75**, 4250 (1995); J. G. Amar and F. Family, Phys. Rev. B **54**, 14 742 (1996).
[17] P. Šmilauer and D. D. Vvedensky, Phys. Rev. B **48**, 17 603 (1993).
[18] Adatoms have a probability $p/4$ of hopping to one of their four neighboring 4FH sites and a probability $1 - p$ of being spontaneously incorporated. It can be shown that this results to a finite diffusion length $\ell_d = a\sqrt{p/(1-p)}$ on a flat terrace, a being the distance between 4FH sites.
[19] M. Copel *et al.*, Phys. Rev. B **42**, 11 682 (1990).